

THE INTERSTELLAR MEDIUM NEAR STARS WITH PECULIAR INTERSTELLAR POLARIZATIONS

JUDITH G. COHEN

Kitt Peak National Observatory*

Received 1976 September 21

ABSTRACT

The properties of the interstellar medium along the line of sight to the small number of stars whose wavelength of maximum interstellar polarization is greater than or equal to 6500 Å are studied. The optical interstellar line measurements reported here confirm the hypothesis that the long λ_{\max} phenomenon occurs in regions where the mean grain size is abnormally large, and that this takes place only in the densest parts of the interstellar medium. The grains grow by accretion from the gas, not by coalescence of previously existing grains. Furthermore, the material accreted in the dense clouds (i.e., the mantle) must have a different chemical composition from the grain core; it must consist of substances composed largely of hydrogen.

Subject headings: interstellar: abundances — interstellar: matter — polarization

I. INTRODUCTION

Two major studies (Serkowski, Mathewson, and Ford 1975, hereafter SMF; Coyne, Gehrels, and Serkowski 1974, hereafter CGS) of the wavelength dependence of interstellar polarization have been completed recently. Their results indicate that the interstellar polarization curve as a function of wavelength for all stars can be fitted by a unique function with one free parameter—the wavelength of maximum polarization (λ_{\max}). The values of λ_{\max} are concentrated in the range 5000 Å to 6500 Å with very few outside this range; only 7% of the stars in SMF's tabulation have $\lambda_{\max} \geq 6500$ Å. Furthermore, only one supergiant is among this group, and its λ_{\max} is 6700 Å. SMF suggest that the few cases of stars with long λ_{\max} (which we shall consider to be $\lambda_{\max} \geq 6500$ Å) are due to the presence of larger than normal grains. It is interesting to note that included in this small group of stars are most of the reddened stars in the Ophiuchus cloud, a region which Cohen (1973) and Carrasco, Strom, and Strom (1973) have already suggested is characterized by larger than normal grains from other lines of evidence. We study this group of stars with long λ_{\max} to determine whether their optical interstellar lines are consistent with the hypothesis of larger grains. Since the metals in the gas must accrete to the grains to increase the mean grain size, we expect that for these stars the optical interstellar lines will prove to be very weak for their reddening. The results agree with this hypothesis, suggesting that the grains grow by accreting mantles from the gas rather than by coalescence of previously existing grains. We also show that most of the stars with long λ_{\max} are located in well-known dark-cloud complexes similar to the Ophiuchus cloud where one

may reasonably expect grain growth owing to high density and ultraviolet shielding.

II. SPECTROSCOPIC OBSERVATIONS

The extremely restricted range of λ_{\max} is shown in Figure 1, which is a plot of P_{\max} against λ_{\max} from the data of SMF and CGS. We concentrate our attention on the few stars which have $\lambda_{\max} \geq 6500$ Å to try to understand the cause of this uncommon behavior. In Table 1 are listed the O and B stars with $\lambda_{\max} \geq 6500$ Å and P_{\max} (the percentage of polarization at λ_{\max}) $> 0.5\%$, where the polarization data are from Table 2 of CGS and Tables 3 and 5 of SMF. Stars with inaccurate values of λ_{\max} or evidence for intrinsic polarization have been omitted. There are three stars (HD 73882, HD 112244, and HD 113034) south of -40° declination which meet these criteria; however, insufficient observational data exist, and these stars are omitted from all further discussions. The stars in the ρ Oph cloud which belong in the long λ_{\max} group (ν Sco, ρ Oph AB, ρ Oph C, ρ Oph D, and HD 147889) are also omitted from Table 1, as complete optical interstellar line observations can be found in Cohen (1973). A few O and B stars whose λ_{\max} was just below the cutoff value of 6500 Å were also observed; they are listed at the bottom of the table. The values of λ_{\max} and P_{\max} in the second and third columns are from CGS and SMF, as are the $B - V$ colors unless otherwise noted.

High-dispersion spectra were obtained at the wavelengths of the Ca II and Na I interstellar doublets. For the Ca II line, the baked IIA-O emulsion was used with the Kitt Peak National Observatory coude auxiliary telescope. Spectra in the yellow region were obtained with the same telescope, using the 098-04 emulsion. For the fainter stars, spectra were obtained on baked IIIa-J plates with the echelle or Cassegrain spectrographs and a Carnegie image tube on the 4 m telescope.

* Operated by the Association of Universities for Research in Astronomy, Inc., under contract with the National Science Foundation.

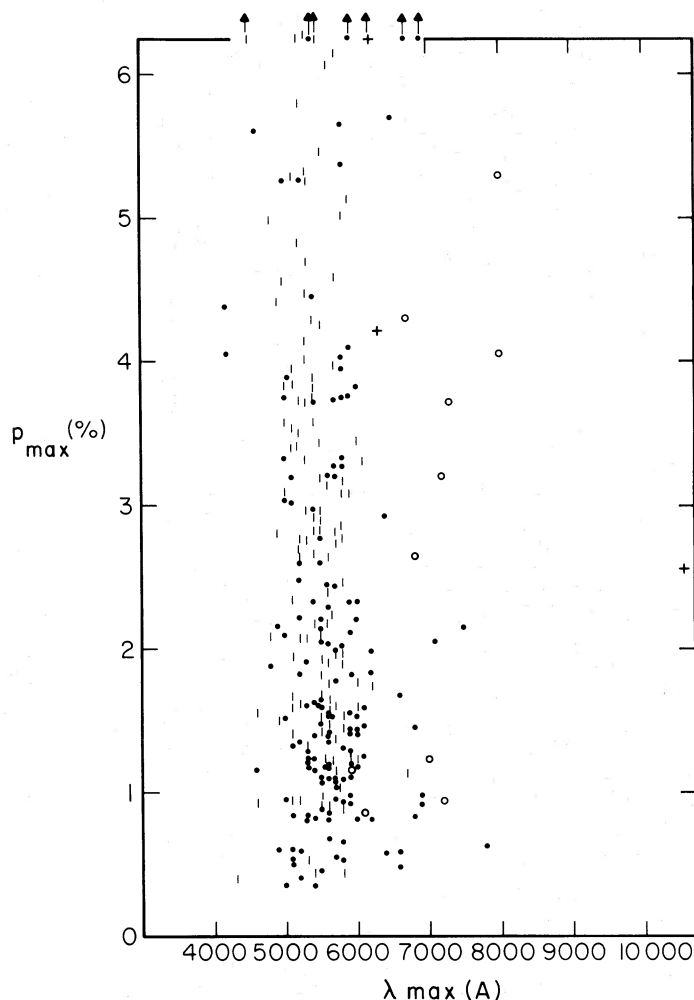


FIG. 1.—A plot of the percentage of maximum interstellar polarization (P_{\max}) versus the wavelength at which the maximum polarization occurs (λ_{\max}). The data are from SMF (1975). *Vertical lines*, supergiant stars (luminosity class I); *circles*, stars in the Ophiuchus cloud; *crosses*, stars in M78; and *dots*, other stars. The stars in CGS with $\lambda_{\max} > 6000 \text{ \AA}$, which are not listed in SMF, are also plotted.

The blue coude auxiliary spectra (which we will call class A and which had mostly dispersions of 13 \AA mm^{-1}) were measured, using a single coordinate oscilloscope Grant machine for the radial velocity of the Ca II interstellar doublet (V_i). The best of the 4 m Cassegrain spectrograph spectra (class C spectra) (dispersion 12 \AA mm^{-1} with an image tube) were also measured for V_i of the Ca II doublet, but the results are not as accurate as in the case of the spectra taken at the coude auxiliary without an image tube. The echelle spectra (class B spectra) taken at 5.1 \AA mm^{-1} were also measured for V_i , using the Na I doublet. The echelle spectra at 12 \AA mm^{-1} and a few of the 4 m Cassegrain spectrograph plates could not be measured accurately. We estimate the errors to be $\pm 4 \text{ km s}^{-1}$ for class A spectra, $\pm 5 \text{ km s}^{-1}$ for class B spectra, and $\pm 8 \text{ km s}^{-1}$ for class C spectra. The four cases for which a velocity is given by Adams (1949) show satisfactory agreement with our measured V_i . These

values of V_i and the error class are listed in the fifth column of Table 1. The distance r_{dm} derived from the color excess and distance modulus is listed in the last column of Table 1. A value of $A_v = 3 E_{B-V}$ was assumed. For a few cases, r_{dm} was also calculated using $A_v = 5 E_{B-V}$, and these values are given in parentheses. A distance r_i is also given, based on the observed V_i corrected to the local standard of rest (LSR) system and using the galactic rotation law

$$V_i^{\text{LSR}} = Ar_i \sin(2l^{\text{II}}).$$

If no value of r_i is given, then the sign of the observed V_i (in the LSR system) is inconsistent with the sign of the predicted V_i^{LSR} .

The spectra were traced using the PDS digital microphotometer. Calibration exposures, exposed and developed simultaneously with the spectra, were used to transform density to intensity. Equivalent widths

TABLE 1
Basic Data for Long λ_{\max} Stars

| Name | λ_{\max} (μ) | P_{\max} (%) | E_{B-V} (mag) | V_i (km s $^{-1}$) | r_i (pc) | r_{dm} (pc) | Nebulosity |
|--------------|-------------------------------|-------------------|--------------------|--------------------------|---------------|------------------|------------|
| HD 36958 | 0.72 | 0.88 | 0.11 | +26.5 A | 900 | 760 | Orion |
| HD 37061 | 0.64 | 1.54 | 0.55 | +25.0 A | 770 | 575 | Orion |
| HD 37903 | 0.71 | 2.04 | 0.37 | + 8.5 A | | 950 | Orion |
| HD 38563 N | 1.03 | 2.55 | 1.47 | | | 910 (230) | M78 |
| HD 40111 | 0.68 | 0.83 | 0.13 | +11.0 A | 620 | 1386 | |
| HD 162978 | 0.68 | 1.46 | 0.36 | - 4.0 A | 2800 | 1056 | L150 |
| HD 163800 | 0.66 | 1.69 | 0.62 | -11.0 A | | 1127 | L215 |
| HD 164740 | 0.67 | 7.35 | 0.90 | +15.0 B | | 3300 (1440) | M8 |
| NGC 2024 #1 | 0.69 | 10.81 | 1.69 | +25 - 5 B | 800 | 1500 (330) | NGC 2024 |
| Other Stars: | | | | | | | |
| HD 36374 | 0.60 | 2.37 | 0.36* | +15.7 A | | 260 | |
| HD 37367 | 0.62 | 0.81 | 0.42 | -29.1 A | | 325 | |
| HD 38051 | 0.61 | 1.25 | 0.58 | +14 C | | 750 | |
| HD 180968 | 0.78† | 0.61† | 0.30‡ | - 7.5 A | 830 | 460 | |
| HD 259440 | 0.62 | 4.05 | 0.85: | +10 C | | 1575 | Rosette |

*B-V from Cohen (unpublished).

†Polarization parameters uncertain.

‡B-V from Crawford, Barnes, and Golson (1971).

were then determined for the interstellar Ca II doublet and the Na I doublet. These measurements are listed in Table 2, where we give the dispersion of the spectra and the number of spectra available for each star in parentheses. Image-tube plates are denoted by roman numerals; direct photographic plates are in arabic numerals. While it is difficult to assign an error to image-tube results, all were treated consistently, and a reasonable estimate is $\pm 15\%$. Particularly uncertain measurements are followed by colons. In a few cases, the weaker line of the Ca II doublet was lost in H ϵ and could not be measured.

III. DISCUSSION

The radial velocities for a few of the stars are in themselves important. The radial velocity in the LSR system of the H II region in NGC 2024 is $+6$ km s $^{-1}$ (± 4) based on the 6584 [N II] line which appears in emission in our stellar spectrum. This is in good agreement with the radial velocities determined from the hydrogen recombination lines and molecular lines observed in the radio (Tucker, Kutner, and Thaddeus 1973). The stellar radial velocity cannot be determined accurately, but it is less than $+6$ km s $^{-1}$, as the

TABLE 2
Interstellar Line Strengths

| Name | Ca II | | | Na I | | |
|--------------|--|---|---|--|---|---|
| | Dispersion (\AA mm $^{-1}$) (No. of Spectra) | W_{λ} (3933) (m \AA) | W_{λ} (3968) (m \AA) | Dispersion (\AA mm $^{-1}$) (No. of Spectra) | W_{λ} (5889) (m \AA) | W_{λ} (5895) (m \AA) |
| HD 36958 | 9 (1) | 100 | | 18 (1+I) | 200 | 135 |
| HD 37061 | 12 (2) | 120 | 70: | 18 (1) | 230 | 195 |
| HD 37903 | 12 (II) | 80 | | 24 (II) | 275 | 165 |
| HD 38563 N | 12 (I) | 190: | | 13 (I) | 240 | 125 |
| HD 40111 | 9 (2) | 160 | 105: | (2) | 350 | 230 |
| HD 162978 | 12 (2) | 190 | 110 | 18 (1) | 330 | 265 |
| HD 163800 | 12 (2) | 240 | 110: | 18 (1) | 460 | 350: |
| HD 164740 | | | | 5 (I) | 310 | 250 |
| NGC 2024 #1 | | | | 5 (I) | 215 | 215 ($v_i = +25$) |
| | | | | | 120 | 60 ($v_i = -5$) |
| Other Stars: | | | | | | |
| HD 36374 | 9 (1) | 145 | | 18 (2) | 260 | 210 |
| HD 37367 | 5 (1) | 200 | 130 | 18 (1) | 270 | 200 |
| HD 38051 | 12 (II) | 235 | | 24 (II) | 400 | 260 |
| HD 180968 | 12 (2) | 95 | 60: | 18 (1) | 280 | 200 |
| HD 259440 | 12 (I) | 380 | 270 | 24 (I) | 865 | 610 |

centroid of the stellar H α absorption profile is to the blue of the narrower nebular H α emission. The distance $r_{am} = 1500$ pc is obtained for NGC 2024 No. 1 using $A_v = 3E_{B-v}$; however, it seems unlikely that the star is that distant. If we adopt the larger ratio of total-to-selective absorption suggested for this region by Johnson and Mendoza (1964), $A_v = 5E_{B-v}$ (which also seems to fit better the colors from 3500 Å to 10 μ m [Grasdalen 1974] for this star), then a distance of 330 pc is obtained, which is very close to that estimated for the dark cloud NGC 2024. That then leaves the problem of the peculiar V_i of the second component. The gas may be in an expanding circumstellar shell around NGC 2024 No. 1 itself, or the relatively large velocity may arise in a shock between the H II region and the dark cloud, or a shock from an extensive stellar wind from the companion to NGC 2024 No. 1 (a star about 2 mag fainter and 5" away), if the companion were a T Tauri star recently formed and blowing away the remnants of the cloud from which it condensed. In the latter case, one could also explain the large infrared excess seen by Grasdalen, while the visual spectrum appears relatively normal. Careful infrared and visual observations of the companion to NGC 2024 No. 1 may clarify this point. Peculiar radial-velocity components in the optical interstellar lines in the η Car region (a similar situation of a dark cloud plus H II regions) have been reported by Walborn and Hesser (1975). HD 164740 (Herschel 36) in M8 does not present such a problem. The nebular emission lines in our spectrum yield a V_i of about $+20$ km s $^{-1}$, while the V_i from the Na I doublet is $+15 \pm 5$ km s $^{-1}$; thus there is no inconsistency here. We also note that HD 37367 is a spectroscopic binary, and the Ca II lines probably originate within the binary system. This could explain the peculiar V_i of -29 km s $^{-1}$ for HD 37367.

The more satisfactory fit of the distance to NGC 2024 No. 1 with the probable distance to the cloud in which it is embedded, using a ratio of total-to-selective absorption (\mathcal{R}) of 5, suggests that we examine the other cases of large reddening to see if similarly abnormal values can be obtained for \mathcal{R} . The distance to M78 (a part of the Orion complex) is 500 pc (Allen 1973), and \mathcal{R} must be 3.9 in order for r_{am} to equal the distance to M78, which agrees well with the value $\mathcal{R} = 3.6$ derived by Strom *et al.* (1975) from infrared photometry. The distance to M8 is 1200 pc (Allen 1973), and the required value of \mathcal{R} to equate the distance of HD 164740 (Herschel 36) to the nebula is 5.4. (SMF derive $\mathcal{R} = 5.5$ from infrared photometry.) While the adopted absolute magnitudes for the embedded stars taken from Allen (1973) may be incorrect, it seems unlikely that they could be too luminous in such a systematic way and that the agreement with \mathcal{R} as derived from infrared photometry could be purely fortuitous.

The explanation suggested by SMF and CGS for the cases of $\lambda_{max} \geq 6500$ Å is that the grains are larger than normal. It is very suggestive that it is precisely among the most reddened of these stars that there is good evidence for a value of \mathcal{R} larger than the canonical value. We now discuss the physical location

of these stars to show that this, too, is consistent with the hypothesis of larger grain size. The Palomar Sky Survey blue plates and the ESO B Survey were examined to determine whether or not each of the stars in Table 1 (plus the three southern stars) was located in a bright nebula or a dark cloud (i.e., a high-density gas). Several of the long λ_{max} stars are located in the Orion Nebula, one each in M78, M8, NGC 2024, L215, and L150 (Lynds 1962). Of the long λ_{max} stars, only two (HD 40111 and HD 112244) are not located in obvious dark clouds or emission regions. Only one of the other stars at the bottom of Table 1 is located in such a region, namely, HD 259440, which lies in the Rosette Nebula and at approximately the same distance. At this point, we must recall that the sample of O and B long λ_{max} stars in Table 1 (plus the three southern stars) is complete except for the stars in the ζ Oph cloud, a well-known, high-density region. Thus the long λ_{max} stars are largely associated with dense clouds (parts of which may be ionized to form the observed emission nebulae). This is again in agreement with the hypothesis that, for the lines of sight to the long λ_{max} stars, the grains are larger than normal, as grain growth is expected to occur most readily in clouds and nebulae owing to the high density and the resultant ultraviolet shielding.

We now consider the optical interstellar lines to see whether they can help substantiate the model developed above. From the equivalent widths given in Table 2, we compute column densities using a curve of growth for a single cloud with a Gaussian velocity distribution. In spite of much valid criticism of this procedure (Nachman and Hobbs 1973), this ought to be fairly accurate for the nearby stars in clouds, as the dominant contribution to the line will be that due to the cloud in which the star is embedded and the column densities are very low. We restrain ourselves from converting these numbers into column densities relative to hydrogen, using the normal value for the thin interstellar medium of N_H/E_{B-v} , because of the possibility that relatively more hydrogen is present in the grains than the gas in dense regions, and also because of uncertainties owing to molecular hydrogen. We therefore list in Table 3 the column density of Ca II and Na I divided by E_{B-v} for each star.

The normal values of $N(\text{Ca II})/N(\text{H I})$ and $N(\text{Na I})/N(\text{H I})$ for the general interstellar medium are -8.7 ± 0.3 and -8.4 ± 0.3 , respectively (Cohen 1975). If the value $N_H/E_{B-v} = 6 \times 10^{21}$ atoms cm $^{-2}$ mag $^{-1}$ (Jenkins and Savage 1974) is used for the general interstellar medium, these values become $N(\text{Ca II})/E_{B-v} = 13.08$ and $N(\text{Na I})/E_{B-v} = 13.38$. It is immediately apparent that many of the values in Table 3 are significantly below those expected for the normal interstellar medium, and in no case are these values exceeded. We thus conclude that the interstellar lines arising from Ca II and Na I are abnormally weak in stars with $\lambda_{max} \geq 6500$ Å, and furthermore, that the cases with the lowest values of $N(\text{Ca II})/E_{B-v}$ and $N(\text{Na I})/E_{B-v}$ are precisely those stars with the largest color excesses.

If we use $\mathcal{D} = 3E_{B-v}/r_{am}$ (kpc) as a crude indication of the mean density along the line of sight to the λ_{max}

TABLE 3
Column Densities

| Star | $N(\text{Ca II})/E(B-V)$ atoms $\text{cm}^{-2} \text{mag}^{-1}$ | $N(\text{Na I})/E(B-V)$ atoms $\text{cm}^{-2} \text{mag}^{-1}$ |
|--------------|--|---|
| HD 36958 | 13.03* | 13.23 |
| HD 37061 | 12.48 | 13.08 |
| HD 37903 | 12.38* | 12.73 |
| HD 38563 N | 12.18* | 11.98 |
| HD 40111 | 13.33 | 13.38 |
| HD 162978 | 12.83 | 13.13 |
| NGC 2024 #1 | --- | 11.58 ($v_i = -5 \text{ km s}^{-1}$) ≈ 12.58 ($v_i = +25 \text{ km s}^{-1}$) |
| HD 163800 | 12.58 | 12.98 |
| HD 164740 | --- | 12.73 |
| Other Stars: | | |
| HD 36374 | 12.63 | 13.03 |
| HD 37367 | 12.88 | 12.88 |
| HD 38051 | 12.63 | 12.78 |
| HD 180968 | 12.73 | 13.03 |
| HD 259440 | 13.03 | 13.03 |

*assumed doublet ratio = 2.0

stars (with 1 being the value for the normal interstellar medium), we may investigate the dependence of the deficiency of Ca II and Na I as a function of density. This is shown in Figure 2, where the Ophiuchus cloud stars have been added (HD 37367 is not plotted here, as it is a spectroscopic binary and the Ca II lines appear to be circumstellar). For purposes of Figure 2, r_{dm} was taken as the distance to the cloud in which the stars are embedded for the ζ Oph stars, HD 38563 N, HD 164740, and NGC 2024 No. 1, but using the value of r_{dm} from Table 1 for these cases would not significantly alter the appearance of Figure 2. The general trend is clearly an increasing deficiency of both Ca II and Na I, as the mean density parameter increases. This is in excellent accord with our model, where grains become larger in dense, dark clouds by accret-

ing mantles from material in the gas, so that λ_{max} increases and the interstellar gas is depleted onto the grains even more than normal. It is difficult to explain the trends seen in Figure 2 as an ionization effect (see the discussion of Cohen 1973) instead of a real variation in depletion of the gas onto the grains.

It is interesting to compare the behavior of M78, whose stars are about 5×10^5 years old (Strom *et al.* 1975), with that of M8, whose stars are about 3×10^6 years old (Walker 1957). In the older region, an O7 star has formed, and the ultraviolet flux from it appears to have prevented the formation of larger grains, blown them away, or evaporated them, since, in spite of a large P_{max} , the value of λ_{max} in HD 164740 is only 6700 Å.

One more calculation must be done to check our

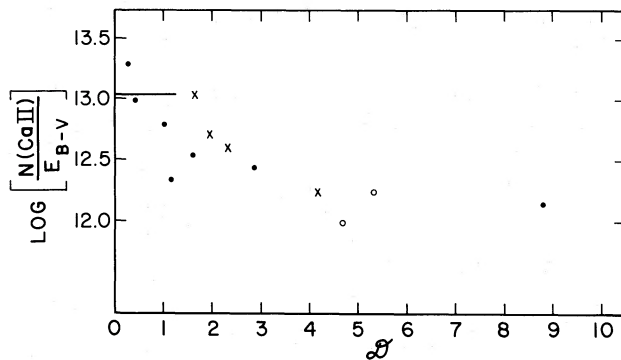


FIG. 2a

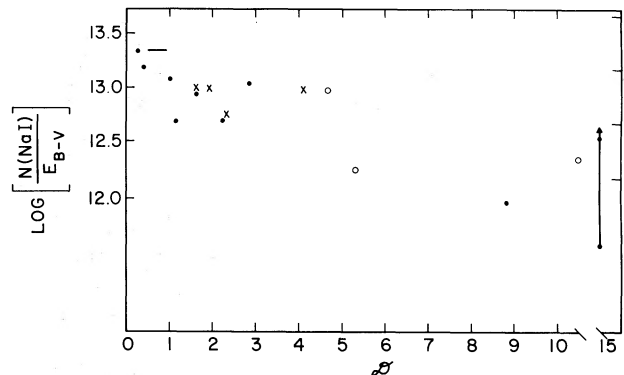


FIG. 2b

FIG. 2a.—A plot of the column density of Ca II divided by the color excess E_{B-V} as a function of \mathcal{D} , a parameter linearly proportional to the mean density along the line of sight. Filled circles, λ_{max} stars of Table 1; open circles, the Ophiuchus cloud stars; crosses, the other stars listed at the bottom of Table 1. The normal thin interstellar medium abundance is indicated by a solid horizontal line.

FIG. 2b.—The same as Fig. 2a for the column density of Na I divided by the color excess E_{B-V} . The two components in NGC 2024 No. 1 are connected by a vertical line.

model, and that is to determine whether or not grains as large as the maximum observed size can be produced if everything in the gas adheres to them. According to Wickramasinghe (1972), λ_{\max} is linearly proportional to the mean grain size multiplied by $(n - 1)$, where n is the refractive index. The largest values of λ_{\max} that have been observed are about $1 \mu\text{m}$ (grains approximately twice normal size). This implies a volume increase (or mass increase, if we assume the density approximately constant) per grain of a factor of 7. Since the normal interstellar gas is already seriously depleted of most of the chemically active heavy elements (Münch 1968; Morton *et al.* 1973; Field 1974), there is not a factor of 7 more of most elements to add to the grain to increase the mean size by such a large amount. This is apparent when one realizes that normally approximately 1% by weight of the interstellar medium is in the form of grains, and that the elements heavier than He are only 1% of the total cosmic material by weight. We are therefore forced to conclude that the mantles which accrete onto grains in dense regions have different chemical compositions from the grain cores, preferably a composition involving as much hydrogen and as little of the heavier elements as possible (such as water ice). (The actual increase in mean grain size required to fit the maximum λ_{\max} value of $1 \mu\text{m}$ will depend on the difference in the index of refraction between the grains of normal size and those which have accreted large mantles; normally n is smaller for grains of high hydrogen content.) The behavior of the 4430 \AA diffuse interstellar line in dense, dark clouds (Snow and Cohen 1974), such as the Ophiuchus region, also implies a qualitative chemical difference in the surface of the grains as compared with less dense regions. Furthermore, the infrared absorption band due to water ice is seen only in dense molecular clouds (Merrill, Russell, and Soifer

1976). Although this may be an optical depth effect, the presence of water ice absorption only in dense clouds tends to add support to the hypothesized difference in chemical composition of the grains in the densest regions of the interstellar medium.

IV. CONCLUSIONS

We summarize here the principal conclusions of our investigation of early-type stars with peculiar interstellar polarization properties.

1. Stars which are selected to have $\lambda_{\max} \geq 6500 \text{ \AA}$ tend to be located in or near the densest regions of the interstellar medium that can be studied optically.

2. The long λ_{\max} stars have abnormally weak interstellar lines of Ca II and Na I for their color excesses. The lowest column densities of Ca II and Na I relative to the color excess E_{B-V} were found in stars located in the densest regions.

3. The most extreme long λ_{\max} stars have a ratio of total-to-selective absorption of approximately 5 based on two independent lines of evidence.

4. All of the above are consistent with the explanation of the long λ_{\max} phenomenon as arising in cases where the mean size of the grains is larger than in the normal interstellar medium, and where grains grow by accretion from the gas rather than from coalescence of previously existing grains.

5. Based on crude theoretical estimates of the behavior of λ_{\max} with the mean grain size, the increase in size required implies that, in the densest regions where the grains are larger, the accreted mantles do not have the same chemical composition as the grain cores, but rather are composed of substances which contain mostly hydrogen, such as water ice.

We thank G. Grasdalen for helpful advice on NGC 2024.

REFERENCES

- Adams, W. S. 1949, *Ap. J.*, **109**, 354.
 Allen, C. W. 1973, *Astrophysical Quantities* (3d ed.; London: Athlone Press).
 Carrasco, L., Strom, S. E., and Strom, K. M. 1973, *Ap. J.*, **182**, 95.
 Cohen, J. G. 1973, *Ap. J.*, **186**, 149.
 ———. 1975, *Ap. J.*, **197**, 117.
 Coyne, G. V., Gehrels, T., and Serkowski, K. 1974, *A.J.*, **79**, 581 (CGS).
 Crawford, D. L., Barnes, J. V., and Golson, J. C. 1971, *A.J.*, **76**, 1058.
 Field, G. B. 1974, *Ap. J.*, **187**, 453.
 Grasdalen, G. L. 1974, *Ap. J.*, **193**, 373.
 Jenkins, E. B., and Savage, B. D. 1974, *Ap. J.*, **187**, 243.
 Johnson, H. L., and Mendoza, E. E. 1964, *Bol. Obs. Tonantzintla y Tacubaya*, **3**, 331.
 Lynds, B. T. 1962, *Ap. J. Suppl.*, **7**, 1.
 Merrill, K. M., Russell, R. W., and Soifer, B. T. 1976, *Ap. J.*, **207**, 763.
 Morton, D. C., Drake, J. F., Jenkins, E. B., Rogerson, J. B., Spitzer, L., and York, D. G. 1973, *Ap. J. (Letters)*, **181**, L103.
 Münch, G. 1968, in *Nebulae and Interstellar Matter*, ed. B. M. Middlehurst and L. H. Aller (Chicago: University of Chicago Press), p. 394.
 Nachman, P., and Hobbs, L. M. 1973, *Ap. J.*, **182**, 481.
 Serkowski, K., Mathewson, D. S., and Ford, V. L. 1975, *Ap. J.*, **196**, 261 (SMF).
 Snow, T. P., and Cohen, J. G. 1974, *Ap. J.*, **194**, 313.
 Strom, K. M., Strom, S. E., Carrasco, L., and Vrba, F. J. 1975, *Ap. J.*, **196**, 489.
 Tucker, K. D., Kutner, M. L., and Thaddeus, P. 1973, *Ap. J. (Letters)*, **186**, L13.
 Walborn, N. R., and Hesser, J. E. 1975, *Ap. J.*, **199**, 535.
 Walker, M. F. 1957, *Ap. J.*, **125**, 636.
 Wickramasinghe, N. C. 1972, in *Interstellar Matter*, ed. Astronomical Institute, University of Basel (Geneva: Geneva Observatory), p. 309.

JUDITH G. COHEN: Kitt Peak National Observatory, P.O. Box 26732, Tucson, AZ 85726